applied sciences

MDPI

Supporting information to: “Theoretical Evaluation of Microwave Ablation Applied on Muscle, Fat and Bone: A Numerical Study”

Cheng Chen [1,&], Ming-An Yu [2,&], Lin Qiu [3], Hongyu Chen [1], Zhenlong Zhao [2], Jie Wu [2], Lili Peng [2], Zhiliang Wang [1], and Ruoxiu Xiao [1,4,*]

1 School of Computer and Communication Engineering, University of Science and Technology Beijing, Beijing China; xiaoruoxiu@ustb.edu.cn
2 Interventional Medicine, China-Japan Friendship Hospital, Beijing, China; yma301@163.com
3 School of Energy and Environmental Engineering, University of Science and Technology Beijing, Beijing, China; qiulin@ustb.edu.cn
4 Institute of Artificial Intelligence, University of Science and Technology Beijing, Beijing, China; xiaoruoxiu@ustb.edu.cn
* Correspondence: xiaoruoxiu@ustb.edu.cn; Tel.: +86-15210326132
& Cheng Chen and Ming-An Yu contributed to this work equally.

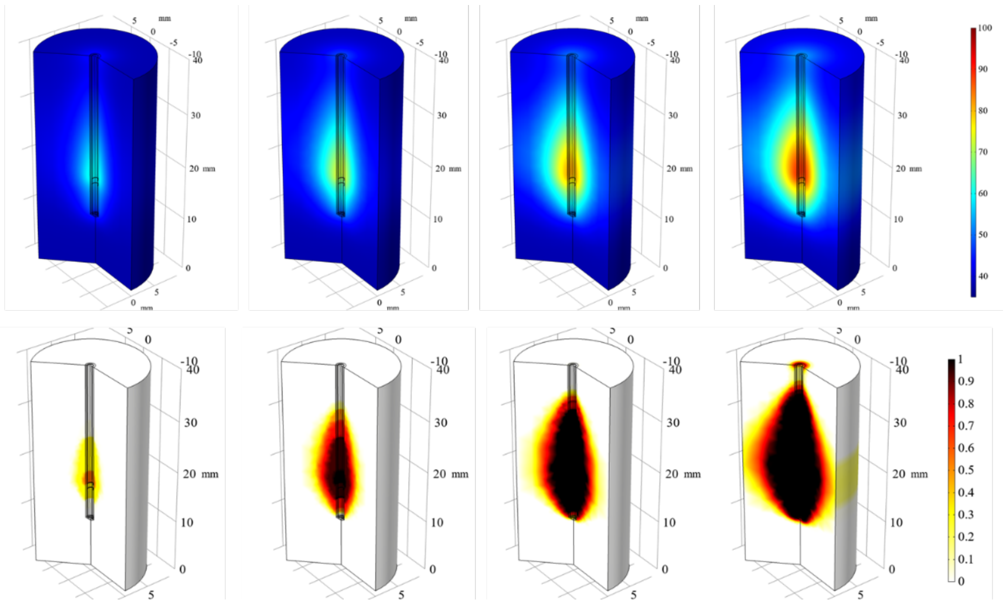

Figure S1. Temperature and damage fraction cloud map using varying thermal conductivity.

Current numerical studies for biological tissues often consider the ideal situation, that is, the fixed parameters [1]. Nevertheless, some parameters vary quite markedly as temperature rises, especially when discussing temperature distribution and temperature-based thermal damage distribution. The temperature change law of thermal conductivity is an essential factor. This section aims to add the muscle’s temperature and damage fraction distribution under the change of thermal conductivity. Since there is no strict public research on muscle’s thermal conductivity and temperature changes, this part is used as a supporting information for follow-up discussion.

Considering that the liver structure is like muscle composition (except for water, protein is the main component). According to the existing public studies of the liver [2], we refer to the law of thermal conductivity change of the liver to simulate the temperature and thermal damage distribution of muscles under the condition of thermal conductivity changes. The law of thermal conductivity change is defined as follows:

$$k(T) = k_0 + 0.0008 \cdot T(^\circ C) \quad \text{(s1)}$$

where, k_0 is the constant thermal conductivity of the muscle at core body temperature.

Keeping the same simulation conditions, under the thermal conductivity change with temperature, Figure s1 shows the muscle model's temperature cloud map and damage fraction cloud map at the 15 s, 30 s, 45 s, and 60 s. During the heating process, the high-temperature area of the muscle gradually appears above the annular groove. Moreover, with time, its heat diffuses outwards with this position as the center. It can be seen from the damage fraction cloud map that the damaged area spreads out in the high temperature zone, and the thermal damage in the high temperature zone is more severe and almost irreversible. Therefore, the distribution law of figure s1 is like the distribution law of figures 3 and 6.

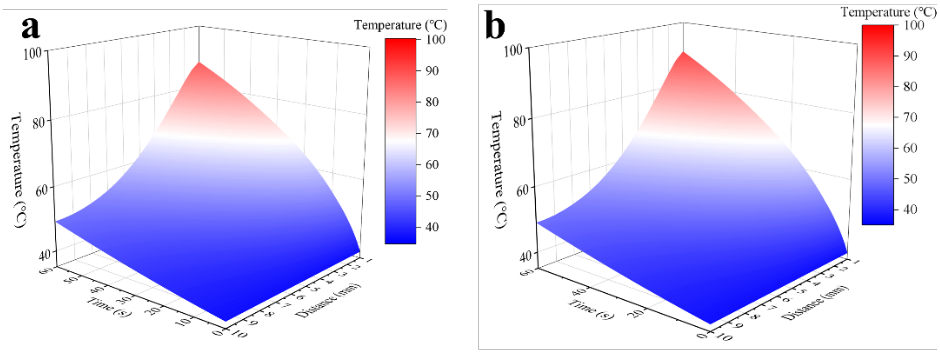

Figure S2. Temperature distribution at the horizontal thermometric sequence of the highest temperature point near ablation antenna. (**a**) Thermal conductivity changes with temperature; (**b**) Constant thermal conductivity

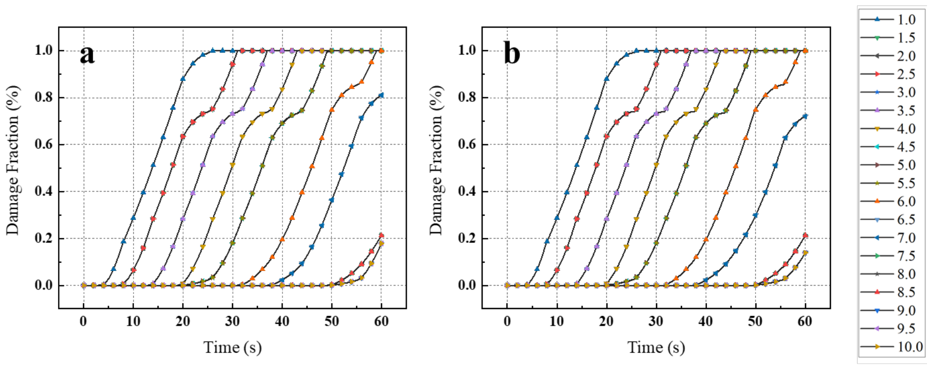

Figure S3. Damage fraction at z=18 mm during 0-60 s. (**a**) Thermal conductivity changes with temperature; (**b**) Constant thermal conductivity

The highest temperature point position of the muscle near the ablation antenna is selected. The point is taken horizontally along this position, and the temperature and damage score of each point in the 0-60s of the entire heating process is collected. Both the highest temperature points are at z=18mm.

Figure S2 shows the changes in temperature at each level overtime when both are at z=18mm. The trends and shapes of the two temperature cloud graphs are the same. The only difference is that the thermal conductivity changes with the increase in temperature, and its heat transfer capacity strengthens with the increase in temperature. The maximum temperature decreases slightly.

Figure S3 records the damage scores. The general trends of them are similar. The damage is mainly concentrated in the ablation antenna needle to the top of the shaft, and the lower part of the shaft is not easily damaged. Even if the damage on the upper part spreads over a large area, the lower part can still maintain a reasonable cell survival rate. From the ablation antenna needle to 18mm, the position is getting closer and closer to its high temperature area. Therefore, the increased rate of damage score and complete damage gradually increases. Considering the change of thermal conductivity with temperature, the increased temperature enhances the heat transfer in the tissue. The location far away from the ablation antenna is more likely to receive heat, resulting in a slight increase in the final damage score and damage rate at a distant location.

Therefore, the thermal conductivity change has little effect on the temperature and thermal damage of muscle tissue, and there is no significant difference in conclusions. Therefore, the ideal model of fixed thermal conductivity has a specific reference when analyzing muscle tissue.

Reference

1. Wu, X.; Liu, B.; Xu, B. Theoretical evaluation of high frequency microwave ablation applied in cancer therapy. Applied Thermal Engineering 2016, 107, 501-507, doi: 10.1016/j.applthermaleng.2016.07.010.
2. Zhang, M.; Zhou, Z.; Wu, S.; Lin, L.; Gao, H.; Feng, Y. Simulation of temperature field for temperature-controlled radio frequency ablation using a hyperbolic bioheat equation and temperature-varied voltage calibration: a liver-mimicking phantom study. Physics in Medicine and Biology 2015, 60, 9455-9471, doi:10.1088/0031-9155/60/24/9455.
3. Ibitoye, A.Z.; Orotoye, T.; Nwoye, E.O.; Aweda, M.A. Analysis of efficiency of different antennas for microwave ablation using simulation and experimental methods. Egyptian Journal of Basic and Applied Sciences 2018, 5, 24-30, doi: 10.1016/j.ejbas.2018.01.005.
4. Macchi, E.G.; Gallati, M.; Braschi, G.; Cigada, A.; Comolli, L. Temperature distribution during RF ablation on ex vivo liver tissue: IR measurements and simulations. Heat and Mass Transfer 2015, 51, 611-620, doi:10.1007/s00231-014-1437-7.
5. Haemmerich, D.; Schutt, D.J. RF Ablation at Low Frequencies for Targeted Tumor Heating: In Vitro and Computational Modeling Results. IEEE Transactions on Biomedical Engineering 2011, 58, 404-410, doi:10.1109/TBME.2010.2085081.